



Lack of antiviral activity of probenecid *in vitro* and in Syrian golden hamsters

Helen J. Box^{1,2†}, Joanne Sharp^{1,2†}, Shaun H. Pennington ³, Edyta Kijak^{1,2}, Lee Tatham^{1,2}, Claire H. Caygill³, Rose C. Lopeman³, Laura N. Jeffreys³, Joanne Herriott^{1,2}, Megan Neary ^{1,2}, Anthony Valentijn^{1,2}, Henry Pertinez^{1,2}, Paul Curley^{1,2}, Usman Arshad^{1,2}, Rajith K. R. Rajoli ^{1,2}, Dirk Jochmans⁴, Laura Vangeel⁴, Johan Neyts⁴, Eric Chatelain⁵, Fanny Escudié ⁵, Ivan Scandale⁵, Steve Rannard^{2,6}, James P. Stewart⁷, Giancarlo A. Biagini³ and Andrew Owen ^{1,2*}

¹Department of Pharmacology and Therapeutics, Institute of Systems, Molecular and Integrative Biology, University of Liverpool, Liverpool L7 3NY, UK; ²Centre of Excellence in Long-acting Therapeutics (CELT), University of Liverpool, Liverpool L7 3NY, UK; ³Centre for Drugs and Diagnostics, Department of Tropical Disease Biology, Liverpool School of Tropical Medicine, Liverpool L3 5QA, UK; ⁴KU Leuven, Department of Microbiology, Immunology and Transplantation, Rega Institute, Laboratory of Virology and Chemotherapy, 3000, Leuven, Belgium and the Global Virus Network (GVN), Baltimore, MD, USA; ⁵Drugs for Neglected Diseases initiative (DNDi), Research and Development, 1202, Geneva, Switzerland; ⁶Department of Chemistry, University of Liverpool, Liverpool L7 3NY, UK; ⁷Department of Infection Biology & Microbiomes, Institute of Infection, Veterinary and Ecological Sciences, University of Liverpool, Liverpool, UK

*Corresponding author. E-mail: aowen@liverpool.ac.uk

†Should be considered as joint first authors.

Received 10 October 2023; accepted 8 November 2023

Objectives: Antiviral interventions are required to complement vaccination programmes and reduce the global burden of COVID-19. Prior to initiation of large-scale clinical trials, robust preclinical data to support candidate plausibility are required. This work sought to further investigate the putative antiviral activity of probenecid against SARS-CoV-2.

Methods: Vero E6 cells were preincubated with probenecid, or control media for 2 h before infection (SARS-CoV-2/Human/Liverpool/REMRQ0001/2020). Probenecid or control media was reapplied, plates reincubated and cytopathic activity quantified by spectrophotometry after 48 h. *In vitro* human airway epithelial cell (HAEC) assays were performed for probenecid against SARS-CoV-2-VoC-B.1.1.7 (hCoV-19/Belgium/reg-12211513/2020; EPI_ISL_791333, 2020-12-21) using an optimized cell model for antiviral testing. Syrian golden hamsters were intranasally inoculated (SARS-CoV-2 Delta B.1.617.2) 24 h prior to treatment with probenecid or vehicle for four twice-daily doses.

Results: No observable antiviral activity for probenecid was evident in Vero E6 or HAEC assays. No reduction in total or subgenomic RNA was observed in terminal lung samples ($P > 0.05$) from hamsters. Body weight of uninfected hamsters remained stable whereas both probenecid- and vehicle-treated infected hamsters lost body weight ($P > 0.5$).

Conclusions: These data do not support probenecid as a SARS-CoV-2 antiviral drug.

Introduction

Many clinical trials have focused upon putative antiviral drugs repurposed either after approval for another indication (e.g. hydroxychloroquine, lopinavir, ivermectin¹⁻⁷) or earlier in development for other viruses (e.g. remdesivir, molnupiravir, nirmatrelvir⁸⁻¹²). The speed at which drugs can be brought forward under the

urgency of a pandemic is a significant advantage of drug repurposing, but this strategy is prone to failure in the absence of robustly conducted and validated preclinical data.

Clinical trials incur significant costs and place additional burden on healthcare systems,^{13,14} and it is important that only candidates that can be robustly justified are studied. Candidates should only be considered worthy of investigation if: (i) the

mechanism of action is plausible and supports the intended use; (ii) the pharmacokinetics (PK) at the proposed dose support that antiviral activity can be achieved in the target population; (iii) reproducible preclinical data are available to demonstrate activity in preclinical models; and (iv) acceptable safety in the target population can be justified at the proposed dose. Although the safety and PK of drugs repurposed after approval for another indication is usually well understood, the impact of the disease should also be considered, particularly when known adverse drug effects may overlap with disease symptomatology. Caution is also required since PK in COVID-19 patients can differ to those of patients with the primary indication.¹⁵ During the pandemic, preclinical models of SARS-CoV-2 infection were developed at unprecedented speed, and data to either support or refute candidacy of repurposing opportunities have been forthcoming.^{16–20} However, cross-validation of preclinical supporting evidence is needed to support progression of a drug from preclinical testing to clinical trials.

Probenecid is a gout treatment for which antiviral activity was reported *in vitro* and in SARS-CoV-2-infected Syrian golden hamsters.²¹ At the time of writing, a clear mechanism of antiviral action of probenecid for SARS-CoV-2 has not been empirically evidenced. However, the low cost, favourable safety profile and wide availability of the drug would advance the implementation of this treatment if antiviral activity can be confirmed. Accordingly, the present study sought to further investigate the putative antiviral activity of probenecid.

Materials and methods

Materials

PBS was purchased from Merck. Male Syrian golden hamsters were purchased from Janvier Labs. Swabs (1 mL Liquid Amies Regular Flocked) were purchased from Appleton Woods. GoTaq[®] Probe 1-Step RT-qPCR System was purchased from Promega. SARS-CoV-2 (2019-nCoV) CDC qPCR Probe Assay, CDC RUO 2019-nCoV_N_Positive Control and the SARS-CoV-2 E SgRNA were purchased from IDT. TRIzol reagent, GlycoBlue[™], Phasemaker[™] tubes, Nanodrop and TURBO DNA-free[™] kit were purchased from Thermo Fisher. A bead mill homogenizer was purchased from Fisher Scientific. Precellys CKMix lysing tubes were purchased from Bertin Instruments. A Chromo4[™] Real-Time PCR Detector was purchased from Bio-Rad. Transmission cages were purchased from Tecniplast UK Ltd. GS-441524 was purchased from Carbosynth (UK).

Viral isolates

SARS-CoV-2 (hCoV-2/human/Liverpool/REMRQ0001/2020; Genbank MW041156) was cultured from a nasopharyngeal swab from a patient.²² SARS-CoV-2 B.1.1.7 (derived from hCoV-19/Belgium/reg-12211513/2020; EPI_ISL_791333, 2020-12-21) was isolated from a nasopharyngeal swab of a traveller returning to Belgium and provided by Prof. Piet Maes, KU Leuven—Rega Institute, Belgium. The B.1.617.2 (Delta variant; hCoV-19/England/SHEF-10E8F3B/2021; GISAID EPI_ISL_1731019) was kindly provided by Prof. Wendy Barclay, Imperial College London, London, UK. The titres of all isolates were confirmed in Vero E6 cells and the sequences of all stocks confirmed.

In vitro Vero E6 cell assay

Seven-point concentration–effect analysis was performed with probenecid in 96-well plates using Vero E6 cells. Cells were preincubated with probenecid or remdesivir (control) at 25.00, 8.33, 2.78, 0.93, 0.31, 0.10 and

0.03 μ M, or control medium at 37°C with 5% CO₂ for 2 h. Preincubation medium was replaced with 50 μ L of minimal medium containing SARS-CoV-2 (moi 0.05), 100 μ L of 2 \times semi-solid medium and then 50 μ L of minimal medium containing probenecid, remdesivir (control) or control medium. Plates were incubated at 37°C with 5% CO₂. After 48 h, paraformaldehyde was added to achieve 4% and the plate incubated for 1 h at room temperature. Cells were stained with crystal violet and washed three times with water. Cytopathic viral activity was determined by measuring absorbance of each well at 590 nm using a Varioskan LUX. Drug activity was expressed as percentage inhibition of viral growth relative to uninfected/untreated control and the infected/untreated control on that plate. Automated analysis was performed to maintain data integrity and objectively assess output. Non-linear regression generated concentration–effect predictions.

In vitro human airway epithelial cell (HAEC) assay

GS-G441524 was used as a positive control, which previously demonstrated robust antiviral activity against SARS-CoV-2.²³ HAECs (Epithelix, Geneva, Switzerland, catalogue no. EP01MD) of bronchial origin from a healthy donor were obtained in air–liquid interphase inserts. The inserts were washed with pre-warmed MucilAir medium (Epithelix, catalogue no. EP04MM) and maintained in 24-well plates, with the same medium at the basal site, at 37°C and 5% CO₂ for at least 4 days before use. On Day 0, the HAECs were pre-treated for 1 h with basal medium with or without compounds, followed by exposure to 100 μ L of SARS-CoV-2 B.1.1.7 inoculum (500 TCID₅₀/mL) from the apical side for 1.5 h, after which the inoculum was removed. The first apical wash with medium was performed 24 h after infection. Every other day from Day 0, subsequent apical washes were collected whereas medium, with or without compound, in the basolateral side of the HAEC culture was refreshed.

For analysis of viral RNA, 5 μ L of apical wash was mixed with 50 μ L of lysis buffer (Cells-to-cDNA[™] II cell lysis buffer, Thermo Fisher Scientific, catalogue no. AM8723), followed by incubation at room temperature for 10 min and then at 75°C for 15 min. Nuclease-free water (150 μ L) was added to the mixture prior to quantitative RT-PCR (RT-qPCR). In the same way a 10-fold serial dilution of corresponding virus stock, with known infectious titre, was extracted. The amount of viral RNA was quantified by RT-qPCR using iTaq universal probes one-step kit (Bio-Rad, catalogue no. 1725141), and a commercial mix of primers for N gene (forward primer 5'-GACCCAAAATCAGCGAAAT-3', reverse primer 5'-TCTGTTACTGCCAGTTGAATCTG-3') and probe (5'-FAM-ACCCCGCATTACGTTTG GTGGACC-BHQ1-3') manufactured at IDT Technologies (catalogue no. 10006606). The reaction consisted of 10 μ L of one-step reaction mix 2 \times , 0.5 μ L of RT, 1.5 μ L of primers and probes mix, 4 μ L of nuclease-free water, and 4 μ L of viral RNA. The RT-qPCR was executed on a LightCycler 96 thermocycler (Roche), starting at 50°C for 15 min and 95°C for 2 min, followed by 45 cycles of 3 s at 95°C and 30 s at 55°C. In the same RT-qPCR, a standard curve was included using the 10-fold serial dilution of the corresponding virus stock with known infectious titre. The Ct was then expressed as TCID₅₀-equivalents of the original virus stock. The results are therefore given as TCID₅₀eq/insert.

In vivo studies

Prior to the start of the study, risk assessments and standard operating procedures were approved by the University of Liverpool Biohazards Sub-Committee and the UK Health and Safety Executive. Animal studies were conducted in accordance with UK Home Office Animals Scientific Procedures Act (ASPA, 1986) under UK Home Office Project Licence PP4715265. Male Syrian golden hamsters (80–100 g; Janvier Labs) were housed in individually ventilated cages with environmental enrichment under specific pathogen-free (SPF) barrier conditions and a 12 h light/dark cycle at 21°C \pm 2°C, with free access to food and water. Hamsters were randomly assigned into three groups of five and acclimatized for

7 days. Subsequently, hamsters were anaesthetized under 3% isoflurane and intranasally inoculated with either PBS (Group 1) or 100 μL of 1×10^3 nCoV19 isolate SARS-CoV-2 Delta variant B.1.617.2 (Groups 2 and 3). Twenty-four hours post-infection (p.i.), hamsters were treated, through intraperitoneal (IP) administration, with vehicle, NaOH solution buffered to pH 7 (Groups 1 and 2) or probenecid in buffered NaOH solution (100 mg/kg; Group 3). Treatment continued twice daily for 48 h p.i. On Day 3 p.i., all animals were ethically euthanized with IP pentobarbitone followed by cardiac puncture.

Quantification of viral load from *in vivo* study samples by qPCR

A portion of lung lobe was homogenized in 1 mL of TRIzol reagent (Thermo Fisher) using a bead mill homogenizer and Precellys CKMix lysing tubes at 3.5 m/s for 30 s. The resulting lysate was centrifuged at 12 000 $\times g$ for 5 min at 4°C. Throat swab medium (260 μL) was added to 750 μL of TRIzol LS reagent. The clear supernatants were transferred to Phasemaker™ tubes and processed as per the manufacturer's instructions to separate total RNA from the phenol-chloroform layer. Subsequently, the recovered RNA was precipitated using GlycoBlue™ according to the manufacturer's instructions, washed and solubilized in RNase-free water. The RNA was quantified using a Nanodrop. Samples were diluted to either 20 000 or 200 ng/mL in 60 μL of RNase-free water. The resulting RNA samples were DNase treated using the TURBO DNA-free™ kit according to the manufacturer's instructions. The DNase-treated RNA was stored at -80°C prior to downstream analysis.

The viral RNA derived from hamster lung was quantified using a protocol adapted from the CDC 2019–Novel Coronavirus (2019–nCoV) Real-Time PCR Diagnostic Panel¹⁷ and a protocol for quantifying the SARS-CoV-2 subgenomic E gene RNA (E SgRNA)¹⁸ using the GoTaq® Probe 1-Step RT-qPCR System (Promega). For quantification of SARS-CoV-2 using the nCoV assay, the N1 primer/probe mix from the SARS-CoV-2 (2019–nCoV) CDC qPCR Probe Assay (IDT) was selected. A standard curve was prepared (1 000 000–10 copies/reaction) via a 10-fold serial dilution of the CDC RUO 2019–nCoV_N_Positive Control (IDT). DNase-treated RNA at 200 ng/mL or dH₂O was added to appropriate wells producing final reaction volumes of 20 μL . The prepared plates were run using a Chromo4™ Real-Time PCR Detector. The thermal cycling conditions for the RT–qPCR reactions were: 1 cycle of 45°C for 15 min, 1 cycle of 95°C for 2 min, followed by 45 cycles of 95°C for 3 s and 55°C for 30 s.

Quantification of SARS-CoV-2 E SgRNA was completed utilizing primers and probes previously described elsewhere¹⁹ and were used at 400 and 200 nM, respectively (IDT), using the GoTaq® Probe 1-Step RT-qPCR System. Quantification of 18S RNA utilized previously described primers and probe sequences,¹⁶ used at 300 and 200 nM, respectively (IDT), using the GoTaq® Probe 1-Step RT-qPCR System. Methods for the generation plan of the 18S and E SgRNA standards have been outlined previously.¹⁸ Both PCR products were serially diluted to produce standard curves in the range of 5×10^5 –5 copies/reaction via a 10-fold serial dilution. DNase-treated RNA at 20 000 ng/mL or dH₂O were added to appropriate wells producing final reaction volumes of 20 μL . The prepared plates were run as per the nCoV assay described above with one change: the final stage of the thermal cycling conditions was 60°C for 30 s. Both N and E SgRNA data were normalized to 18S data for subsequent quantitation.

Quantification of viral load from *in vivo* study by plaque assay

Vero E6 plaque assays were performed for quantification of plaque formation within individual samples. A portion of lung lobe was placed in screw-top microcentrifuge tubes containing a single stainless-steel bead cooled to 4°C. A 500 μL aliquot of EMEM (Gibco; 670086) was added to each microcentrifuge tube and the lung tissue homogenized using a TissueLyser LT (QIAGEN, 85600) for approximately 4–5 min at 50 Hz.

Microcentrifuge tubes were centrifuged at 2000 rpm for 5 min at room temperature. The homogenized tissue supernatant was collected, and stored at -80°C . Homogenized samples were thawed, diluted in EMEM (1:4, 1:20, 1:100, 1:500, 1:2500 and 1:125 000) and layered over confluent Vero E6 cells in 100 μL volumes, in triplicate, in 96-well plates. Semi-solid medium (100 μL) was then added to each well. Plates were incubated at 37°C with 5% CO₂. After 72 h, paraformaldehyde was added to each well to achieve a final concentration of 4% and the plate incubated for 1 h at room temperature. The medium was removed, cells were stained with crystal violet and washed three times with water. The number of plaques in each well were enumerated at the highest countable concentration. The average value was used to calculate the concentration of each sample in viral plaque-forming units (PFU).

Statistical analysis

An unpaired *t*-test was used to compare differences in body weight between probenecid-treated and vehicle-treated groups on Day 3 p.i. using R (v.4.1.2)²⁴

Results

In vitro Vero E6 cell assay

Seven-point concentration–response analysis was performed in triplicate with three independent biological replicates. All plates passed quality control. The control compound, remdesivir, generated a robust four-parameter fit (Figure 1): EC₅₀ = 2.43 μM , EC₉₀ = 9.39 μM , E_{max} = 98.86 and hillslope = 1.80. No detectable activity was observed for probenecid at any concentration up to 25 μM (Figure 1a).

In vitro HAEC assay

A previously optimized HAEC model²³ was used to assess antiviral activity of probenecid versus the parental form of remdesivir, GS-441524. As presented in Figure 1(b), TCID₅₀ values observed in probenecid-treated cells directly mimic those obtained from untreated controls through the course of infection, whereas the parental form of remdesivir suppressed viral replication with levels of antiviral activity observed in previous models using this compound.²³

In vivo hamster model of SARS-CoV-2 infection

All data generated from *in vivo* investigations are reported in accordance with the updated ARRIVE 2.0 guidelines.²⁵ Hamsters were inoculated with virus and 24 h p.i. were treated with probenecid, (IP 100 mg/kg twice daily) for four doses before being ethically euthanized. Figure 2 shows animal weight relative to baseline (Day 0, prior to SARS-CoV-2 inoculation). All animals displayed moderate weight loss 24 h following infection (4%–7% of body weight) regardless of treatment. Mean body weight remained relatively consistent in uninfected animals throughout the study (Figure 2).

To determine the viral load in animals infected with SARS-CoV-2 and dosed with either vehicle control or probenecid, total RNA was extracted from the lung samples harvested on Day 3 p.i. Viral replication was quantified using RT–qPCR to measure total and subgenomic viral RNA relative to the E gene (sgE) as a proxy. These data are illustrated in Figure 3. There was no apparent reduction in either total lung or sgE RNA for probenecid-treated animals

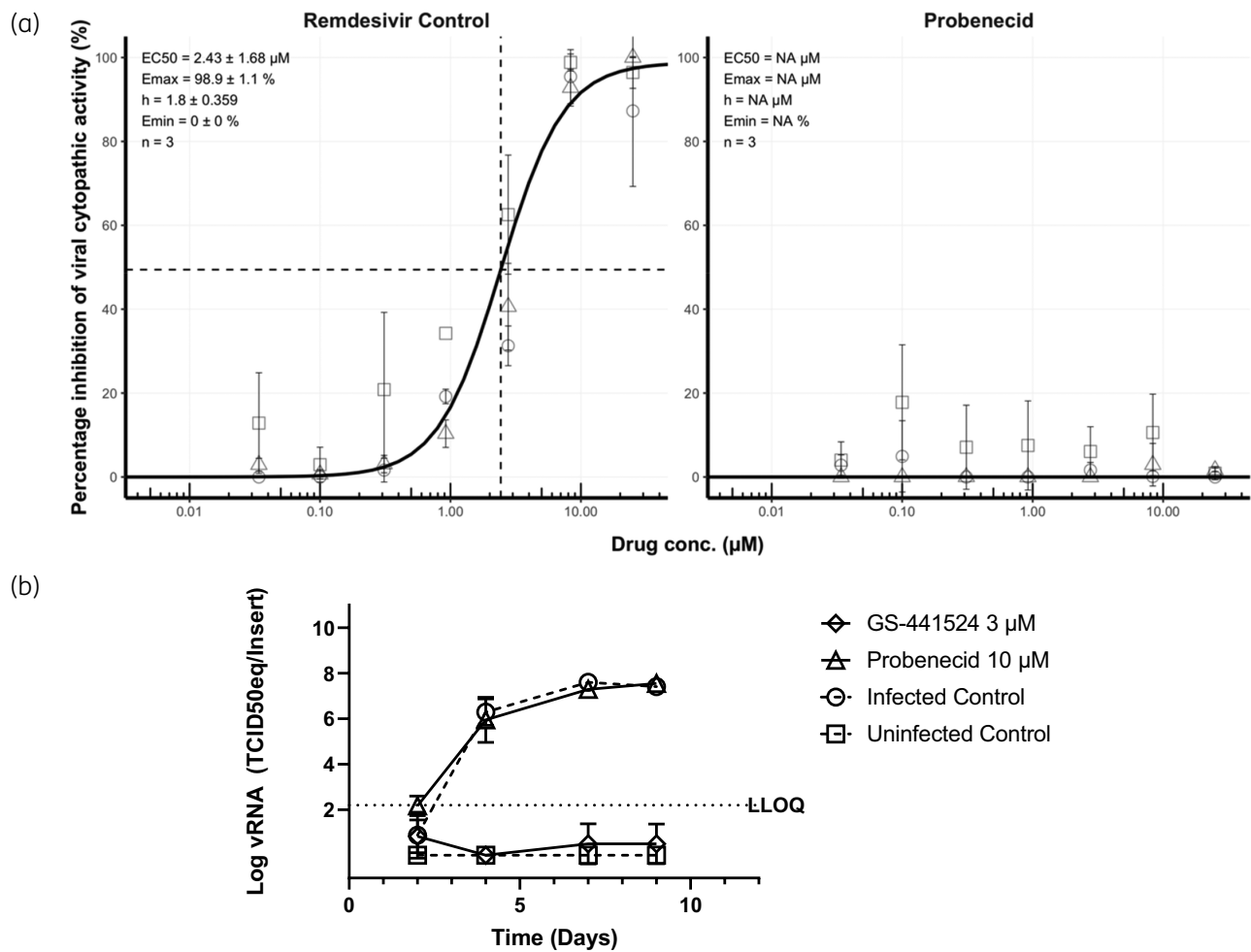


Figure 1. (a) Concentration–effect relationship for the inhibition (%) of SARS-CoV-2 cytopathic activity for remdesivir and probenecid. Non-linear regression using an E_{max} model was performed on data taken from three independent biological replicates to generate concentration–effect predictions (solid black lines). EC_{50} values, hillslope and replicate number (n) are shown. Dashed lines represent the EC_{50} . Squares, diamonds and circles represent individual biological replicates and error bars represent standard deviation calculated from technical triplicates. (b) GS-441524, the parental form of remdesivir, but not probenecid, inhibits SARS-CoV-2 replication in HAEC cultures. Viral RNA in apical washes was determined and mean viral load, converted to equivalent $TCID_{50}$ values based on a standard curve using a virus stock with known titre, and standard deviation is shown. LLOQ, lower limit of quantification in the RT-qPCR as derived from the standard curve.

compared with infected controls ($P > 0.5$). RNA levels for uninfected control samples were below the assay limit of detection (Figure 3). The concentration of PFU per mL of terminal lung samples from SARS-CoV-2 infected animals treated with either vehicle or probenecid was also measured (Figure 4).

Discussion

Repurposed agents usually exert their activity via fortuitous similarity in a target or a secondary mechanism of action, which is often poorly understood. Accordingly, a repurposed drug cannot necessarily be expected to exhibit levels of potency that can be achieved through development of a mechanism-based inhibitor. Nonetheless, drugs such as remdesivir, molnupiravir and nirmatrelvir have shown efficacy in COVID-19, demonstrating the utility of drug repurposing for candidates with a plausible mechanism of action and robust supporting preclinical evidence.

The speed at which preclinical methodologies were developed in the first years of the pandemic is laudable but substantive interlaboratory differences in assay conditions and outcomes are evident. For the most part, concordant overall outcomes have been achieved despite subtle differences in the methodology employed, and overarching conclusions have been consistent. To confidently progress a molecule to clinical evaluation, activity needs to be reproducibly demonstrated, and resilient to subtle differences in methodology. The presented data do not support probenecid as an antiviral treatment for COVID-19, and demonstrate that significant inhibition of SARS-CoV-2 infection is not achieved at dosages where efficacy was previously reported.²¹

Plasma and tissue-site protein binding is known to impact the likelihood of success for some, but not all, drug therapies and should be carefully considered when interpreting candidacy of putative antiviral interventions.²⁶ It is important to note that

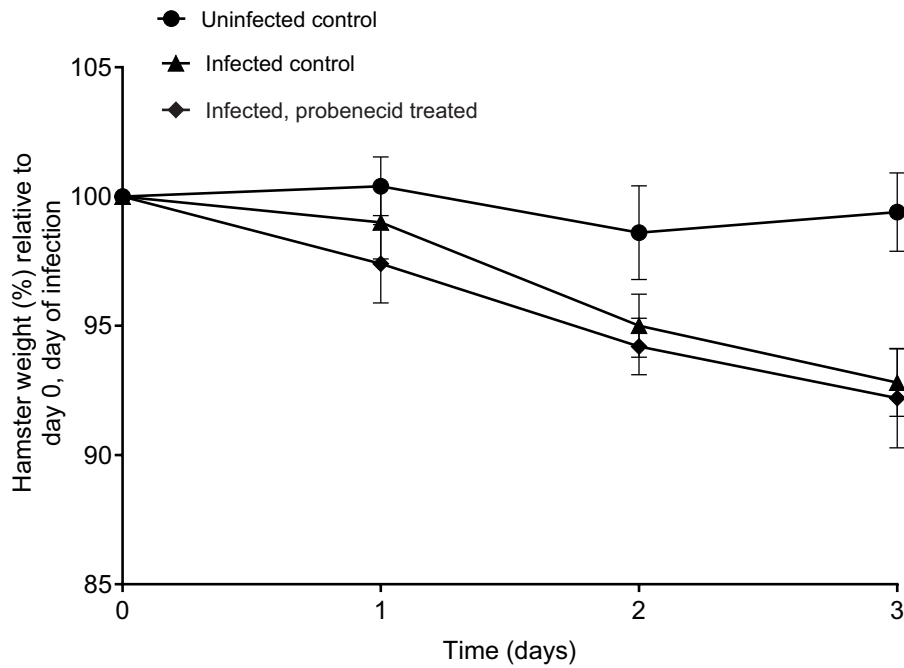


Figure 2. Average body weight data p.i. Error bars represent the standard deviation between individual animal weights.

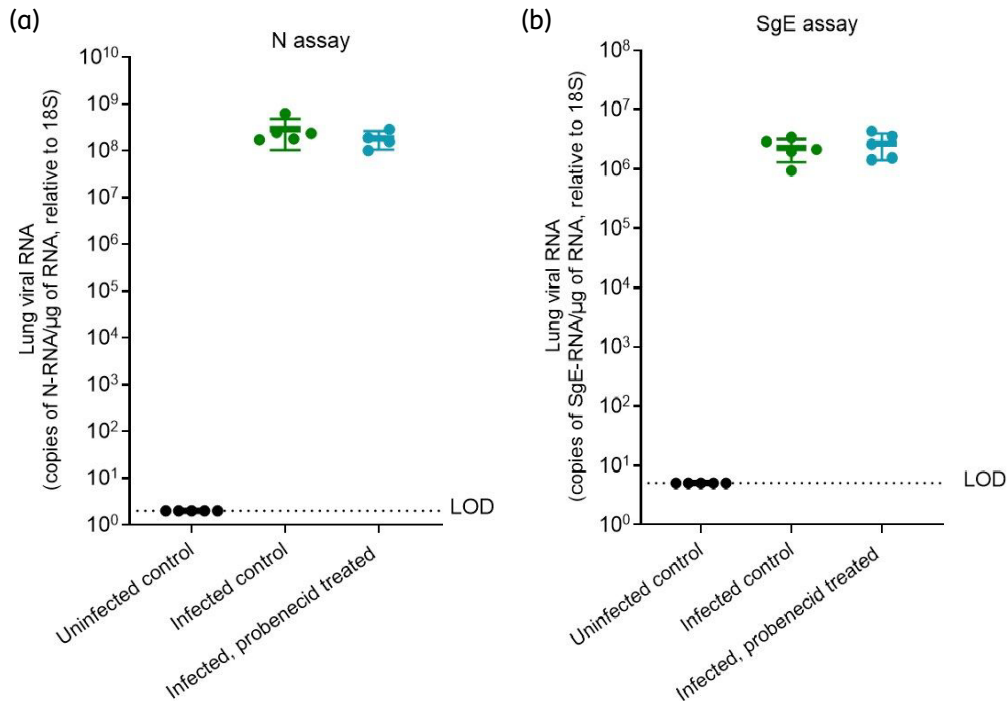


Figure 3. Lung viral RNA normalized to the total RNA (a) and 18 S subunit (b) in untreated controls and SARS-CoV-2-infected animals, treated with vehicle or probenecid. Error bars represent standard deviation between samples obtained from individual animals. Limit of detection (LOD) is set to $y=5$ (SgE assay) and $y=2$ (N assay) as lowest possible standards in assays.

proposed target C_{max}/EC_{90} ratios for probenecid against SARS-CoV-2 in humans are yet to be investigated and that neither the current study, nor previous studies, empirically investigated the consequences of protein binding directly for probenecid.

OAT3 (SLC22) has been proposed as a host target for probenecid activity against influenza A.²⁷ However, the role of OAT3 in SARS-CoV-2 replication has not been empirically investigated and differences in the OAT3 expression across different cell lines

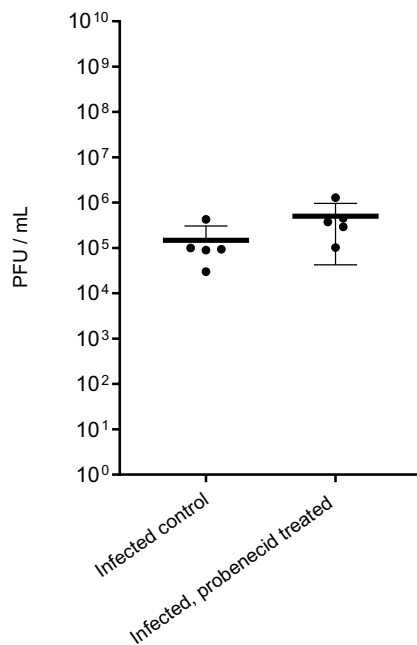


Figure 4. Concentration (pfu/mL) in terminal lung samples from SARS-CoV-2-infected animals, treated with vehicle ($n=5$) or probenecid ($n=5$). Error bars represent standard deviation of values obtained for individual animals.

is unexplored. Probenecid also remains unexplored clinically for influenza and efficacy in influenza is therefore also currently uncertain. The combination of probenecid with oseltamivir was investigated in healthy volunteers in 2005 (NCT00304434), but this study was not premised upon an anticipated antiviral contribution of probenecid.²⁸ More recently, probenecid was demonstrated to down-regulate ACE2 expression in a renal cortical cell line but this mechanism has not been investigated in lung.²⁹ An anti-inflammatory mechanism of action for probenecid has also been suggested via targeting the pannexin-1 gene (*PANX1*), but disease-modifying activity in the absence of an antiviral effect is beyond the scope of the current manuscript.³⁰

Evidence from Vero E6 cell and HAEC assays is presented, which were conducted independently by two separate labs with two independently procured supplies of probenecid. Probenecid did not exert antiviral activity against SARS-CoV-2 Pango lineage B or alpha variant in either study. Differences in the duration of *in vitro* experiments may influence the outcome depending upon the mechanism of action, but robust antiviral drugs should be resilient to these differences. Furthermore, the absence of virological efficacy in the animal experiments were concordant with the presented *in vitro* data.

Positive controls based upon remdesivir were successfully employed for the presented *in vitro* studies, with a clear parallel demonstration of their antiviral activities. However, differences in carboxylesterase activity between rodents and humans render remdesivir an unsuitable control for small animal studies. The lack of a positive control in the reported hamster study is a limitation, but the successful application of the hamster model in demonstrating effectiveness of interventions has been published by the investigators.^{31,32} The presented data therefore do not

support the use of probenecid as an antiviral drug for SARS-CoV-2 infection.

Acknowledgements

We thank Ralph Tripp and Jackelyn Crabtree at the University of Georgia for highly constructive discussions to understand differences in methodology. We thank Tina Van Buyten and Niels Cremers for excellent technical assistance with the HAEC cultures. Part of this project was carried out and funded through DNDi under support by the Wellcome Trust Grant ref: 222489/Z/21/Z through the COVID-19 Therapeutics Accelerator.

Funding

With the exception of data from human airway epithelial cells, the current work was funded by Unitaid (2020-38-LONGEVITY). Human airway epithelial cell assays were carried out and funded through DNDi under the support by the Wellcome Trust (Grant ref: 222489/Z/21/Z) through the 'COVID-19 Therapeutics Accelerator'. A.O. acknowledges funding by Wellcome Trust (222489/Z/21/Z), EPSRC (EP/R024804/1; EP/S012265/1) and National Institute of Health (NIH) (R01AI134091; R24AI118397). J.P.S. acknowledges funding from the Medical Research Council (MRC) (MR/W005611/1, MR/R010145/1), BBSRC (BB/R00904X/1; BB/R018863/1; BB/N022505/1) and Innovate UK (TS/V012967/1). G.A.B. acknowledges support from the Medical Research Council (MRC) (MR/836 S00467X/1) and the UK Research and Innovation (UKRI) Strength in Places Fund (SIPF 20197).

Transparency declarations

A.O. and S.R. are Directors of Tandem Nano Ltd and co-inventors of patents relating to drug delivery. A.O. has been co-investigator on funding received by the University of Liverpool from ViiV Healthcare and Gilead Sciences in the past 3 years unrelated to COVID-19. A.O. has received personal fees from Gilead and Assembly Biosciences in the past 3 years, also unrelated to COVID-19. S.R. has received research funding from ViiV and AstraZeneca and consultancy from Gilead not related to the current paper. No other conflicts are declared by the authors.

References

- 1 Reis G, Moreira Silva EADS, Medeiros Silva DC *et al*. Effect of early treatment with hydroxychloroquine or lopinavir and ritonavir on risk of hospitalization among patients with COVID-19. *JAMA Network Open* 2021; **4**: e216468. <https://doi.org/10.1001/jamanetworkopen.2021.6468>
- 2 Axfors C, Schmitt AM, Janiaud P *et al*. Mortality outcomes with hydroxychloroquine and chloroquine in COVID-19 from an international collaborative meta-analysis of randomized trials. *Nat Commun* 2021; **12**: 2349. <https://doi.org/10.1038/s41467-021-22446-z>
- 3 Self WH, Semler MW, Leither LM *et al*. Effect of hydroxychloroquine on clinical status at 14 days in hospitalized patients with COVID-19. *JAMA* 2020; **324**: 2165. <https://doi.org/10.1001/jama.2020.22240>
- 4 Horby PW, Mafham M, Bell JL *et al*. Lopinavir-ritonavir in patients admitted to hospital with COVID-19 (RECOVERY): a randomised, controlled, open-label, platform trial. *Lancet* 2020; **396**: 1345–52. [https://doi.org/10.1016/S0140-6736\(20\)32013-4](https://doi.org/10.1016/S0140-6736(20)32013-4)
- 5 Group RC, Horby P, Mafham M *et al*. Effect of hydroxychloroquine in hospitalized patients with Covid-19. *N Engl J Med* 2020; **383**: 2030–40. <https://doi.org/10.1056/NEJMoa2022926>
- 6 Griffiths GO, Fitzgerald R, Jaki T *et al*. AGILE: a seamless phase I/IIa platform for the rapid evaluation of candidates for COVID-19 treatment: an

- update to the structured summary of a study protocol for a randomised platform trial letter. *Trials* 2021; **22**: 487. <https://doi.org/10.1186/s13063-021-05458-4>
- 7** Bryant A, Lawrie TA, Fordham EJ. Ivermectin for prevention and treatment of COVID-19 infection: a systematic review, meta-analysis, and trial sequential analysis to inform clinical guidelines. *Am J Ther* 2021; **28**: e434–60. <https://doi.org/10.1097/MJT.0000000000001402>
- 8** Beigel JH, Tomashek KM, Dodd LE *et al.* Remdesivir for the treatment of Covid-19—final report. *N Engl J Med* 2020; **383**: 1813–26. <https://doi.org/10.1056/NEJMoa2007764>
- 9** Jayk Bernal A, Gomes Da Silva MM, Musungaie DB *et al.* Molnupiravir for oral treatment of Covid-19 in nonhospitalized patients. *N Engl J Med* 2022; **386**: 509–20. <https://doi.org/10.1056/NEJMoa2116044>
- 10** Singh RSP, Toussi SS, Hackman F *et al.* Innovative randomized phase I study and dosing regimen selection to accelerate and inform pivotal COVID-19 trial of nirmatrelvir. *Clin Pharmacol Ther* 2022; **112**: 101–11. <https://doi.org/10.1002/cpt.2603>
- 11** ClinicalTrials.gov. EPIC-HR: Study of Oral PF-07321332/Ritonavir Compared With Placebo in Nonhospitalized High Risk Adults With COVID-19. 2021. <https://classic.clinicaltrials.gov/ct2/show/NCT04960202>.
- 12** ClinicalTrials.gov. The Safety of Molnupiravir (EIDD-2801) and Its Effect on Viral Shedding of SARS-CoV-2 (END-COVID). 2021. <https://clinicaltrials.gov/study/NCT04405739>.
- 13** Johnston SC, Rootenberg JD, Katrak S *et al.* Effect of a US National Institutes of Health programme of clinical trials on public health and costs. *Lancet* 2006; **367**: 1319–27. [https://doi.org/10.1016/S0140-6736\(06\)68578-4](https://doi.org/10.1016/S0140-6736(06)68578-4)
- 14** Park JJH, Mogg R, Smith GE *et al.* How COVID-19 has fundamentally changed clinical research in global health. *Lancet Glob Health* 2021; **9**: e711–e20. [https://doi.org/10.1016/S2214-109X\(20\)30542-8](https://doi.org/10.1016/S2214-109X(20)30542-8)
- 15** Alvarez JC, Moine P, Davido B *et al.* Population pharmacokinetics of lopinavir/ritonavir in Covid-19 patients. *Eur J Clin Pharmacol* 2021; **77**: 389–97. <https://doi.org/10.1007/s00228-020-03020-w>
- 16** Clark JJ, Sharma P, Bentley EG *et al.* Naturally-acquired immunity in Syrian Golden Hamsters provides protection from re-exposure to emerging heterosubtypic SARS-CoV-2 variants B.1.1.7 and B.1.351. *bioRxiv* 2021; <https://www.biorxiv.org/content/10.1101/2021.03.10.434447v1>.
- 17** Djidrovski I, Georgiou M, Hughes GL *et al.* SARS-CoV-2 infects an upper airway model derived from induced pluripotent stem cells. *Stem Cells* 2021; **39**: 1310–21. <https://doi.org/10.1002/stem.3422>
- 18** Hiscox JA, Khoo SH, Stewart JP *et al.* Shutting the gate before the horse has bolted: is it time for a conversation about SARS-CoV-2 and antiviral drug resistance? *J Antimicrob Chemother* 2021; **76**: 2230–3. <https://doi.org/10.1093/jac/dkab189>
- 19** Neary M, Box H, Sharp J *et al.* Evaluation of intranasal nafamostat or camostat for SARS-CoV-2 chemoprophylaxis in Syrian golden hamsters. *bioRxiv* 2021; <https://www.biorxiv.org/content/10.1101/2021.07.08.451654v1>.
- 20** Rajoli RKR, Pertinez H, Arshad U *et al.* Dose prediction for repurposing nitazoxanide in SARS-CoV-2 treatment or chemoprophylaxis. *Br J Clin Pharmacol* 2021; **87**: 2078–88. <https://doi.org/10.1111/bcp.14619>
- 21** Murray J, Hogan RJ, Martin DE *et al.* Probenecid inhibits SARS-CoV-2 replication in vivo and in vitro. *Sci Rep* 2021; **11**: 18085. <https://doi.org/10.1038/s41598-021-97658-w>
- 22** Patterson EI, Prince T, Anderson ER *et al.* Methods of inactivation of SARS-CoV-2 for downstream biological assays. *J Infect Dis* 2020; **222**: 1462–7. <https://doi.org/10.1093/infdis/jiaa507>
- 23** Do TND, Donckers K, Vangeel L *et al.* A robust SARS-CoV-2 replication model in primary human epithelial cells at the air liquid interface to assess antiviral agents. *Antiviral Res* 2021; **192**: 105122. <https://doi.org/10.1016/j.antiviral.2021.105122>
- 24** R Core Team. R: a language and environment for statistical computing. 2020. <https://www.r-project.org/>.
- 25** Percie Du Sert N, Hurst V, Ahluwalia A *et al.* The ARRIVE guidelines 2.0: updated guidelines for reporting animal research. *PLoS Biol* 2020; **18**: e3000410. <https://doi.org/10.1371/journal.pbio.3000410>
- 26** Boffito M, Back DJ, Flexner C *et al.* Toward consensus on correct interpretation of protein binding in plasma and other biological matrices for COVID-19 therapeutic development. *Clin Pharmacol Ther* 2021; **110**: 64–8. <https://doi.org/10.1002/cpt.2099>
- 27** Perwitasari O, Yan X, Johnson S *et al.* Targeting organic anion transporter 3 with probenecid as a novel anti-influenza A virus strategy. *Antimicrob Agents Chemother* 2013; **57**: 475–83. <https://doi.org/10.1128/AAC.01532-12>
- 28** Holodniy M, Penzak SR, Straight TM *et al.* Pharmacokinetics and tolerability of oseltamivir combined with probenecid. *Antimicrob Agents Chemother* 2008; **52**: 3013–21. <https://doi.org/10.1128/AAC.00047-08>
- 29** Sinha S, Cheng K, Schaffer AA *et al.* *In vitro* and *in vivo* identification of clinically approved drugs that modify ACE2 expression. *Mol Syst Biol* 2020; **16**: e9628. <https://doi.org/10.15252/msb.20209628>
- 30** Tripp RA, Martin DE. Repurposing probenecid to inhibit SARS-CoV-2, influenza virus, and respiratory syncytial virus (RSV) replication. *Viruses* 2022; **14**: 612. <https://doi.org/10.3390/v14030612>
- 31** Brevini T, Maes M, Webb GJ *et al.* FXR inhibition may protect from SARS-CoV-2 infection by reducing ACE2. *Nature* 2023; **615**: 134–42. <https://doi.org/10.1038/s41586-022-05594-0>
- 32** Huo J, Mikolajek H, Le Bas A *et al.* A potent SARS-CoV-2 neutralising nanobody shows therapeutic efficacy in the Syrian golden hamster model of COVID-19. *Nat Commun* 2021; **12**: 5469. <https://doi.org/10.1038/s41467-021-25480-z>